

wave result when all "distorting potentials" were set equal to zero. These two codes agreed to better than 1%.

The results of Fig. 1 confirm the claim of Ref. 2 that this process can be understood with conventional second-order theory. Finite-range effects are 20 to 40%, depending on the scattering angle. Thus, finite-range theory would be needed only for a detailed study. Future plans for the method outlined here include adding the second-order term to the finite-range DWBA ( $p, t$ ) results of Ref. 8 and to the ( $^{18}\text{O}$ ,  $^{16}\text{O}$ ) calculations of Charlton.<sup>11</sup>

The author would like to acknowledge useful conversations with D. Robson, F. Petrovich, and J. Philpott.

†Work supported in part by the National Science Found-

ation under Grants No. NSF-GU-2612, NSF-GJ-367, and NSF-GP-41834X.

\*Present address: University of California, Lawrence Berkeley Laboratory, Nuclear Chemistry Division, Berkeley, Calif. 94720.

<sup>1</sup>P. D. Kunz and E. Rost, *Bull. Am. Phys. Soc.* **17**, 902 (1972).

<sup>2</sup>N. B. de Takacsy, *Nucl. Phys.* **A231**, 243 (1974).

<sup>3</sup>V. Managoli and D. Robson, to be published.

<sup>4</sup>H. Segawa, K.-I. Kubo, and A. Arima, *Phys. Rev. Lett.* **35**, 357 (1975).

<sup>5</sup>A. M. Lane and D. Robson, *Phys. Rev.* **185**, 1403 (1969).

<sup>6</sup>C. Bloch, *Nucl. Phys.* **4**, 503 (1957).

<sup>7</sup>L. A. Charlton, *Phys. Rev. C* **8**, 146 (1973).

<sup>8</sup>L. A. Charlton, *Phys. Rev. C* **12**, 351 (1975).

<sup>9</sup>W. W. True, *Phys. Rev.* **168**, 1388 (1968).

<sup>10</sup>W. A. Lanford, Cyclotron Laboratory, Michigan State University, Annual Report, 1972 (unpublished); W. A. Lanford and J. B. McGrory, *Phys. Lett.* **45B**, 238 (1973).

<sup>11</sup>L. A. Charlton, *Nucl. Phys.* **A241**, 144 (1975).

## Infrared-Radio-Frequency Two-Photon and Multiphoton Lamb Dips for $\text{CH}_3\text{F}$

S. M. Freund,\* M. Römheld,† and T. Oka

*Herzberg Institute of Astrophysics, National Research Council of Canada, Ottawa, Ontario, Canada*

(Received 15 May 1975)

Inverse Lamb dips caused by two-photon and multiphoton processes of infrared and radio-frequency radiations have been observed for methyl fluoride in a  $\text{CO}_2$  laser cavity. The observations reveal interesting characteristics of the line shape and fine structures of Lamb dips which are explained by using Shimizu's theory. Analysis of the fine structure leads to identification of velocity-tuned multiphoton processes.

We report observations of infrared (IR)-radio-frequency two-photon and multiphoton Lamb dips which are caused by couplings of various multiphoton processes. Two types of processes relevant to our discussion are shown in Fig. 1.

The IR-rf two-photon processes are shown in Figs. 1(a) and 1(b); one rf quantum is (a) added to or (b) subtracted from the IR quantum through nonlinearities of molecular transition processes. In general more than one quantum of rf radiation can be added or subtracted. Such multiphoton processes are well known in microwave spectroscopy<sup>1</sup> and Mössbauer spectroscopy<sup>2</sup> where the Doppler broadening is small. We observe such processes in the infrared region by using Lamb-dip spectroscopy. By utilizing stabilized lasers, the two-photon Lamb dips provide us with a convenient means to perform infrared spectroscopy with the absolute accuracy and resolution of mi-

crowave spectroscopy.

Infrared multiphoton processes, which we call *velocity-tuned three-photon processes*, are shown in Figs. 1(c) and 1(d). They are caused by com-

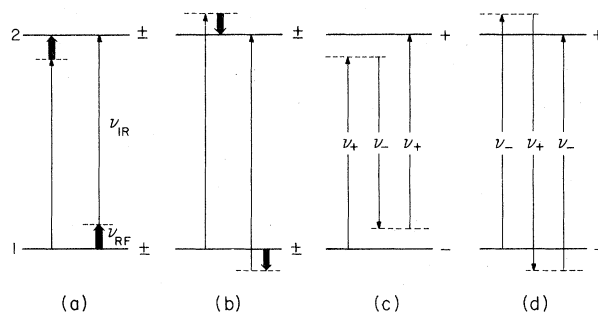


FIG. 1. Energy-level schemes (a), (b), for IR-rf two-photon processes and (c), (d), for velocity-tuned three-photon processes.

binations of IR radiations Doppler-shifted up ( $\nu_+$ ) and Doppler-shifted down ( $\nu_-$ ) with frequencies  $\nu_{\pm} = \nu_1(1 \pm v/c)$ . The resonance conditions with a molecular transition at  $\nu_0$  are

$$\nu_{\pm} - \nu_{\mp} + \nu_{\pm} = \nu_1(1 \pm 3v/c) = \nu_0. \quad (1)$$

Therefore, if the saturation condition is met, the velocity-tuned three-photon processes burn holes in the velocity profile of molecules at one-third the velocities  $\pm v_0$  at which normal single-photon processes burn holes. In general velocity-tuned  $(2l+1)$ -photon processes burn holes at velocities  $\pm v_0/(2l+1)$ . Radiative processes similar to these have been considered in theoretical work on the line shape of Lamb dips.<sup>3-5</sup> Although they were shown to affect the line shapes of Lamb dips, a clear identification of them requires some coupling with other radiative processes. The present experiment reveals the velocity-tuned three-photon processes through couplings with the IR-rf two-photon processes.

The transition moments (in the unit of angular frequency) for the two processes are obtained by perturbation treatment as<sup>6,7</sup>

$$M_2 = \frac{\langle\langle 1 | \vec{\mu}_p \cdot \vec{E}_r | 1 \rangle - \langle 2 | \vec{\mu}_p \cdot \vec{E}_r | 2 \rangle \rangle \langle 1 | \vec{\mu}_v \cdot \vec{E}_l | 2 \rangle}{2\hbar^2 \omega_r} \quad (2)$$

and

$$M_3 = 9 \langle 1 | \vec{\mu}_v \cdot \vec{E}_l | 2 \rangle^3 / 16\hbar^3 (\omega_0 - \omega_l)^2, \quad (3)$$

where  $\vec{E}_r$  and  $\vec{E}_l$  are the electric fields of the rf and the IR laser radiation, respectively,  $\vec{\mu}_p$  and  $\vec{\mu}_v$  are the permanent dipole moment and the vibrational transition moment, respectively, and  $\omega_r = 2\pi\nu_r$  is the applied rf frequency. Equation (2) indicates that the levels 1 and 2 in Figs. 1(a) and 1(b) must have nonzero diagonal Stark matrix element and thus be of double parity; symmetric-top molecules such as  $\text{CH}_3\text{F}$  satisfy this condition. The minus sign in the parentheses shows a destructive interference between the two processes in each of Figs. 1(a) and 1(b). Thus for the worst case of parallel, Q-branch transitions with  $\vec{E}_r \parallel \vec{E}_l$  ( $\Delta J = 0, \Delta K = 0, \Delta M = 0$ ),  $M_2$  is very small in spite of the fact that an individual two-photon process may have a large transition moment. A configuration  $\vec{E}_r \perp \vec{E}_l$  is preferred for such transitions. Using typical values for our experimental conditions ( $E_r \sim 50$  V/cm,  $E_l \sim 200$  V/cm,  $\mu_p = 1.86$  D,  $\mu_v \sim 0.1$  D, direction cosine  $\sim 1/\sqrt{3}$ , and pressure broadening of 40 kHz), we find that the IR-rf two-photon processes and the velocity-tuned IR three-photon processes may saturate

$\text{CH}_3\text{F}$  gas of 2 mTorr up to  $\nu_r \sim 1$  GHz and  $|\nu_l - \nu_0| \sim 50$  MHz.

The experiment was done in the cavity of a  $\text{CO}_2$  laser oscillating in the 9.4- $\mu\text{m}$  band. The absorption cell was a coaxial 50- $\Omega$  transmission line of 66 cm in length terminated at one end with a dummy load. It was sealed with NaCl windows at the Brewster angle and was placed inside the laser cavity near the grating. The rf radiation of about 10 W was frequency modulated at 10 kHz and swept by a saw-tooth voltage. Lamb dips were detected as sharp variations of the laser output power.

Examples of two-photon and multiphoton Lamb dips are shown in Fig. 2. These dips are caused by a set of R-branch rotation-vibration transitions ( $J = 5 \leftarrow 4, K \leftarrow K, K = 4, 3, 2, 1$ ) for the  $\nu_3$  fundamental band of  $^{13}\text{CH}_3\text{F}$ , which lie within 300 MHz of the  $P(32)$  line of the  $\text{CO}_2$  laser in the 9.4- $\mu\text{m}$  region. The frequency of the  $K = 4$  transition is higher than that of the laser line and the frequencies of the  $K = 3, 2, 1$  transitions are lower. This can be easily checked by observing shifts of the resonant rf frequencies when the laser frequency is manually tuned. The  $K = 0$  transition was not observed because the levels have single parity. We have also observed the  $J = 3 \leftarrow 3, K = 3$  and 2 transitions for  $^{13}\text{CH}_3\text{F}$  by using the  $P(40)$  line and the  $J = 12 \leftarrow 12, K = 3$  and 2 transitions for  $^{12}\text{CH}_3\text{F}$  by using the  $P(20)$  line. The observed rf frequencies for the two-photon Lamb dips, together with accurate frequencies of the  $\text{CO}_2$  laser

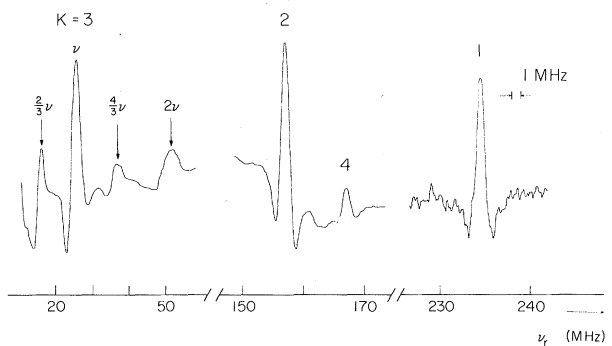


FIG. 2. Observed IR-rf two-photon and multiphoton Lamb-dip signals. The lines correspond to the  $J = 5 \leftarrow 4$  transition of the  $\nu_3$  fundamental of  $^{13}\text{CH}_3\text{F}$  with  $K = 1, 2, 3, 4$ . The sample pressure was 2 mTorr and the time constant for the detection was 300 msec. The fine structure associated with the  $K = 3$  line is due to cross couplings of IR single-photon and IR-rf two-photon processes for  $2\nu$  and IR three-photon and IR-rf two-photon processes for  $2\nu/3$  and  $4\nu/3$ , respectively.

lines,<sup>8</sup> provide us with frequencies of the infrared vibration-rotation transitions with a high accuracy. The results of such measurements have been included in an extensive analysis of the  $\nu_3$  band of  $\text{CH}_3\text{F}$ .<sup>9</sup> Many other Lamb dips have been observed but as yet have not been assigned. We believe that they correspond to either high- $J$  ( $J \geq 10$ ) or hot-band transitions.

Our observation revealed two unexpected features of multiphoton Lamb dips: (i) When the rf frequency was of the order of the Doppler width ( $\sim 30$  MHz) the two-photon Lamb dips at  $\nu_r = \nu \equiv |\nu_i - \nu_0|$  were accompanied by satellite lines at  $\nu_r = 2\nu/3$ ,  $4\nu/3$ , and  $2\nu$  (see the  $K=3$  lines in Fig. 2 where  $\nu_i - \nu_0 = 25.8$  MHz). When  $\nu_i$  was manually varied they moved together keeping the frequency ratio constant. (ii) For weaker two-photon Lamb dips, for which  $\nu = |\nu_i - \nu_0|$  is much larger than the Doppler width, the dips were of dispersion shape (note that the signals in Fig. 2 represent derivatives of dips because of the frequency modulation). For stronger Lamb dips for which  $\nu$  is smaller, the line shape varied between the Lorentzian absorption form and the dispersion form depending on the rf power and the sample pressure. Shimizu<sup>10</sup> has recently developed a theory for two-photon Lamb dips in which he solved a density-matrix equation for molecules interacting with two traveling optical radiation fields and an rf field. We use his solutions to explain our results qualitatively.

Lamb dips are caused when a group of molecules with a certain velocity component are in resonance with both of the oppositely traveling optical radiations  $\nu_+$  and  $\nu_-$ . For most of the IR-rf two-photon Lamb dips in which  $\nu = |\nu_i - \nu_0|$  is much larger than the Doppler width (such as  $K=4$ , 2, and 1 signals in Fig. 2), this condition is met only for molecules with  $v=0$  and  $\nu_+ + \nu = \nu_- + \nu = \nu_i + \nu = \nu_0$  (we assumed  $\nu_i < \nu_0$ ). However when  $\nu$  is of the order of the Doppler width, the condition for Lamb dip is met also by molecules with nonzero velocities. Figure 3 illustrates various couplings of IR single-photon, IR-rf two-photon, and velocity-tuned IR three-photon processes. The Lamb dip at  $\nu_r = 2\nu$  is caused by molecules with the velocity  $kv/2\pi = \pm \nu$  through couplings of IR single-photon ( $\nu_{\pm}$ ) and IR-rf two-photon ( $\nu_{\mp} \mp 2\nu$ ) processes. This dip has a linewidth double that of the center dip at  $\nu_r = \nu$  as expected from the theoretical formula given later. The Lamb dips at  $2\nu/3$  and  $4\nu/3$  are caused by molecules with  $kv/2\pi = \pm \nu/3$  through couplings of velocity-tuned IR three-photon ( $\nu_{\pm} - \nu_{\mp} + \nu_{\pm}$ ) and IR-rf two-

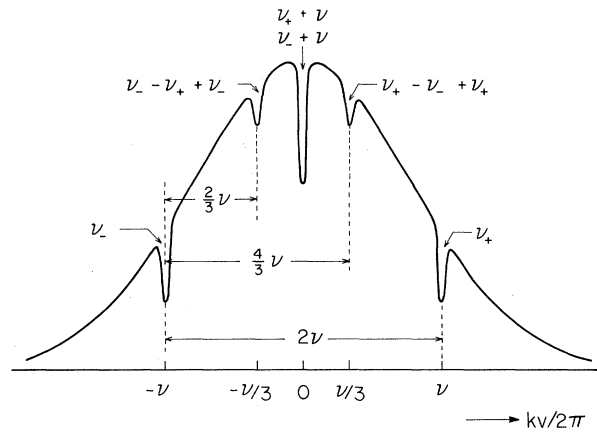


FIG. 3. The Maxwellian velocity profile of molecules in the laser cavity. The IR-rf two-photon processes  $\nu_{\pm} + \nu$  interact with molecules with zero velocity. The IR single-photon processes  $\nu_{\pm}$  and the IR-rf two-photon processes  $\nu_{\mp} \pm 2\nu$  interact with molecules with velocities  $kv = \pm 2\nu$ . The velocity-tuned three-photon processes  $\nu_{\pm} - \nu_{\mp} + \nu_{\pm}$  and the IR-rf two-photon processes  $\nu_{\mp} \pm 4\nu/3$  and  $\nu_{\mp} \pm 2\nu/3$  interact with molecules with velocities  $kv = \pm 2\nu/3$ . Additional holes burned by higher IR multiple-photon processes at  $kv = \pm 2\nu/(2l+1)$  are not shown in the figure.

photon ( $\nu_{\pm} \mp 4\nu/3$ ,  $\nu_{\pm} \mp 2\nu/3$ ) processes. These results provide the first experimental verification of the velocity-tuned multiphoton processes.

Even when  $\nu$  is much larger than the Doppler width, a multiple structure is observed, if the rf matrix element in Eq. (2) is comparable to  $\hbar\nu_r$ . This was experienced in our observation of the  $J=3 \leftarrow 3$ ,  $K=3$  line of  $^{13}\text{CH}_3\text{F}$  where  $\nu_i - \nu_0 = 233.6$  MHz. Using a configuration in which the laser electric field is perpendicular to the rf field to avoid the destructive interference, we observed more than twenty dips at frequencies  $\nu/n$  and  $\nu/(n+\frac{1}{2})$  ( $n=2, 3, \dots, 10$ ). This demonstrates many multiphoton processes of the rf radiation. In general, Shimizu's theory indicates<sup>10</sup> that a multiphoton Lamb dip occurs whenever a condition of the form

$$l\nu_+ - (l \pm 1)\nu_- + m\nu_r = \mp \nu_0 \quad (4)$$

is fulfilled by two sets of integers ( $l, m$ ) and ( $l', m'$ ). It follows that resonances may occur at rf frequencies

$$\begin{aligned} \nu_r &= 2j\nu/n; \\ j &= l' - l, \quad n = 2m'l - 2m'l' \pm m' \mp m. \end{aligned} \quad (5)$$

All our observations are clearly special cases of this general condition.

The line shape of the two-photon Lamb dips can be discussed by considering the  $\nu_r$  dependence of molecular susceptibility.<sup>10</sup> Recently, Shimizu's formulation has been modified<sup>11</sup> by using the "dressed" atom formalism.<sup>12</sup> This formalism gives the susceptibility<sup>7</sup>

$$\chi = - \frac{i\pi\mu_v^4 E_i^2 N(\frac{1}{2}(n-q)\omega_r)}{2\hbar^3} \sum_{m,n,q} J_m(z) J_n(z) J_{m-n+q}(z) J_q(z) \frac{1}{(n-m)\omega_r + i\gamma_0} \frac{1}{2(\omega_i - \omega_0) + (n-q)\omega_r + 2i\gamma_{12}}, \quad (6)$$

where  $J_m(z)$  are the Bessel functions with  $z = 2x_r/\omega_r = [ \langle 1 | \vec{\mu}_p \cdot \vec{E}_r | 1 \rangle - \langle 2 | \vec{\mu}_p \cdot \vec{E}_r | 2 \rangle ] / \hbar\omega_r$ ,  $N(u) = (N/\sqrt{\pi}u_0) \exp[-(u/u_0)^2]$  is the Maxwellian velocity distribution with  $u = kv$ ,  $\gamma_0$  and  $\gamma_{12}$  are the damping coefficients for the diagonal and off-diagonal elements of the density matrix, respectively, and the summations over integers  $m$ ,  $n$ , and  $q$  go from  $-\infty$  to  $+\infty$ . This formula is obtained from the third-order term in the perturbation solution of the density-matrix equation and includes all combinations of  $\nu_{\pm} + n\nu_r$  processes.<sup>13</sup> The Lamb dip at  $\nu_r = \nu$  is obtained by setting  $n+q=2$  in Eq. (6). Using the approximation  $J_n(z) \sim (z/2)^n/n!$ , we find

$$\chi_{\alpha} = \frac{2\pi i \mu_v^2 M_2^2}{\hbar(\omega_i - \omega_0)} \frac{N(0)}{\omega_i + \omega_r - \omega_0 + i\gamma_{12}} \quad \text{for } m=0 \quad (7)$$

and

$$\chi_{\beta} = - \frac{2\pi i \mu_v^2 M_2^2}{\hbar(\omega_i - \omega_0)} \left( \frac{|x_r|^2}{\gamma_0(\omega_i - \omega_0)} \right) \frac{N(0)}{\omega_i + \omega_r - \omega_0 + i\gamma_{12}} \quad \text{for } m=1. \quad (8)$$

$\chi_{\alpha}$  and  $\chi_{\beta}$  correspond to Shimizu's fifth-order and seventh-order terms, respectively. The shape of  $\chi_{\beta}$  is the same as that of the normal inverse Lamb dip [which is obtained by setting  $m=n=q=0$  in Eq. (6)], and the absorption (imaginary) part of  $\chi_{\beta}$  has the normal Lorentzian absorption shape. However, because of an extra  $i$  in  $\chi_{\alpha}$ , the imaginary part of  $\chi_{\alpha}$  has a dispersion shape. Since  $\chi_{\alpha}/\chi_{\beta} = |\omega_i - \omega_0| \gamma_0 / |x_r|^2$ ,  $\chi_{\alpha}$  dominates for large  $|\omega_i - \omega_0|$  and large  $\gamma_0$ , whereas for

small  $|\omega_i - \omega_0|$  and small  $\gamma_0$ ,  $\chi_{\beta}$  dominates. This explains the observed dependence of the two-photon Lamb dip on experimental conditions.

We would like to thank F. Shimizu for many clarifying discussions and A. E. Douglas, A. R. W. McKellar, and J. Reid for reading the manuscript.

\*Present address: Optical Physics Division, National Bureau of Standards, Washington, D. C. 20234.

†Present address: Abteilung für physikalische Chemie, Universität Ulm, D-79 Ulm, Germany.

<sup>1</sup>S. H. Autler and C. H. Townes, Phys. Rev. **100**, 703 (1955).

<sup>2</sup>N. D. Heiman, L. Pfeiffer, and J. C. Walker, Phys. Rev. Lett. **21**, 93 (1968).

<sup>3</sup>S. Haroche and F. Hartmann, Phys. Rev. A **6**, 1280 (1972).

<sup>4</sup>J. H. Shirley, Phys. Rev. A **8**, 347 (1973).

<sup>5</sup>S. Stenholm, private communication.

<sup>6</sup>T. Oka and T. Shimizu, Phys. Rev. A **2**, 587 (1970).

<sup>7</sup>T. Oka, in Proceedings of the Summer School of Theoretical Physics, Les Houches, France, 1975 (to be published).

<sup>8</sup>F. R. Petersen, D. G. McDonald, J. D. Cupp, and B. L. Danielson, Phys. Rev. Lett. **31**, 573 (1973).

<sup>9</sup>S. M. Freund, G. Duxbury, M. Römheld, J. T. Tiedje, and T. Oka, J. Mol. Spectrosc. **52**, 38 (1974).

<sup>10</sup>F. Shimizu, Phys. Rev. A **10**, 950 (1974).

<sup>11</sup>S. Stenholm and E. Arimondo, private communication.

<sup>12</sup>See, for example, C. Cohen-Tannoudji and S. Haroche, J. Phys. (Paris) **30**, 125, 153 (1969).

<sup>13</sup>The velocity-tuned multiphoton processes are not included in this expression.